NEW 1.4 CELL RF PHOTOINJECTOR DESIGN FOR HIGH BRIGHTNESS BEAM GENERATION*

E. Pirez†, J. Maxson, P. Musumeci
Department of Physics and Astronomy, UCLA, Los Angeles, California 90095, USA
D. Alesini, INFN/LNF, Frascati (Roma), Italy

Abstract

The new electromagnetic and mechanical designs of the S-band 1.4 cell photoinjector are discussed. A novel fabrication method is adopted to replace the brazing process with a clamping technique achieving lower breakdown probability. The photoinjector is designed to operate at a 120MV/m gradient and an optimal injection phase of 70° to improve the extraction field by a factor of 1.9 compared to standard 1.6 cell designs with the same peak field. New geometries and features are implemented to improve beam quality for the demand of high brightness beam applications.

INTRODUCTION

For decades radiofrequency (RF) photoinjectors have been the state-of-the-art in terms of high brightness electron sources. They have played a key role in the development of applications such as short wavelength high gain free electron lasers, ultra-fast electron diffraction, inverse Compton scattering, high power THz generation, among others [1–4]. Although several improvements in photoinjector design have been made over the years, the achieved beam brightness is at least five orders of magnitude lower than the theoretical quantum limit for a fully coherent electron source [5]. Significant improvements on beam brightness must be made to further advance high brightness beam applications.

Improving the beam brightness can be done through different methods. These include minimizing the velocity spread of the electrons during photo-emission by either fine-tuning the laser wavelength [6–9] or modifying the characteristics (e.g. work function) of the photocathode [10]. In this paper we will focus on improving beam brightness by increasing the accelerating electric field E_0 the electrons see as they are emitted from the cathode surface, the extraction field. A higher extraction field has several advantages. Particles quickly accelerate away from the cathode reducing the space charge effects that limit peak brightness. It allows for very high current densities from a small area on the photocathode simultaneously reducing the initial emittance.

How the beam brightness scales with the extraction field depends on what definition one uses as many exist in literature [11]. But regardless of the operating regime, maximizing the extraction field at the cathode achieves brighter beams [12–14]. Increasing the peak field involves significant redesign of the RF structures and resolving fundamental material breakdown issues. A simple alternative is to limit the phase slippage due to the fact that the photo-emitted particles are not relativistic. The optimal phase (to reach maximum energy and minimum energy spread) for launching particles in typical 1.6 cell RF guns is close to 30 degrees and much lower than 90 degrees so that the launch field is significantly smaller than the peak achievable field in the gun [15]. Without a drastic redesign of RF photoinjectors, the optimal launch phase can be increased by simply shortening the first cell which minimizes the slippage leading to a higher extraction field.

* Work supported by NSF grant 145583
† eylenepirez@gmail.com

DESIGN OF THE 1.4 CELL PHOTOGUN

The new RF design is based on the design of the 1.6 cell RF structure developed by the SPARC lab of the National Institute of Nuclear Physics (LNF-INFN) [16]. The 1.6 cell photoinjector is currently operating at the Pegasus lab at UCLA at a gradient of 120MV/m. Inspired by the 1.6 cell photoinjector design and fabrication techniques, we have developed a new 1.4 cell photoinjector with a shortened first cell to improve extraction field and therefore increasing beam brightness. In this section we discuss further improvements to the electromagnetic and mechanical design.

Typical 1.6 photoinjectors have an optimal launching phase of $25° - 35°$ depending on the input RF power. The 1.6 cell photoinjector has a first cell of 36.45mm optimal launching phase of 30°. The 1.4 cell photoinjector first cell has a length of d_{half} = 22mm which gives an optimal launching phase of 70°. The higher launching phase increased the extraction field by a factor of $\sin(70°)/\sin(30°) = 1.9$.

In Fig.1a, we show the energy dependence on the injection phase for the 1.6 and the 1.4 cell structure at a 120MV/m gradient. The optimal launching phase is the one for which the maximum output energy is achieved. The 1.4 cell photoinjector has a lower output energy than the SPARC photoinjector due to the shortening of the accelerating region. Many applications of high brightness beams are not critically affected by final electron beam energy. In Fig. 1b, we

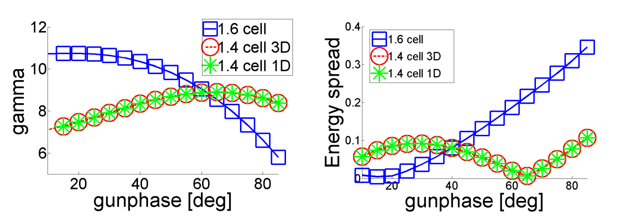

(a) (b)

Figure 1: Comparison between the 1.6 cell (3D map) and the 1.4 cell (1D and 3D maps) photoinjector. (a) Gamma vs. phase. (b) Energy spread.

Copyright © 2016 CC-BY-3.0 and by the respective authors

show the energy spread as a function of injection phase. The 1.4 cell photogun exhibits a lower energy spread than the 1.6 cell gun. The minimum of the energy spread is obtained at $65 - 70°$ as expected.

The electromagnetic design of the cavity have been optimized using Ansys HFSS simulations [17]. The cavity has adopted the SPARC elliptical irises design with an axis ratio of $b/a = 2$ to reduce the surface electric field with respect to the cathode peak field. The iris is now located at z=22mm, see Fig. 2a. The iris diameter is 36mm which is larger than in typical photoinjectors. This large diameter allows for a 50.1 MHz separation between the 0 mode and the π mode. A large mode separation is preferred when operating with short RF pulses as it avoids simultaneous excitation of both modes which can have a negative impact on the beam dynamics. The π mode has a resonance at 2.856GHz as shown in Fig. 2b.

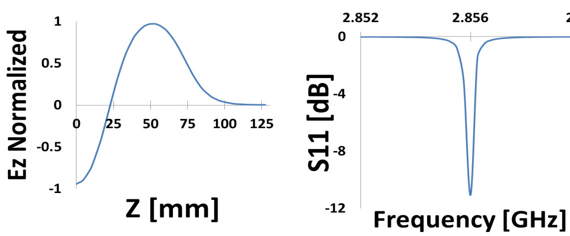

(a) (b)

Figure 2: (a) Ez vs. z (b) S11 coefficient at resonance frequency, f_{π}.

Unlike the 1.6 cell cavity, the full cell of the 1.4 cell cavity does not posses cylindrical symmetry. A new geometry has been adopted [18]. The cross section of the full cell is the intersection of 2 circles, $r_{circle} = 47.3325$mm, with their centers located at an offset,$\Delta y = 4.4$mm, from the central axis of the gun. Two flat planes truncate the cell at a 5mm offset from the point where the circles meet, see Fig. 3. This new full cell geometry reduces the quadrupole moment

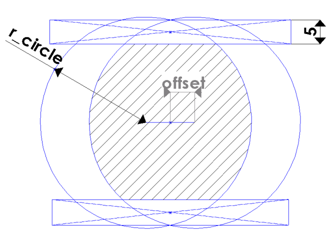

Figure 3: Full cell cross section geometry.

along the central axis. An approximation of the quadrupole moment A(z) can be written as [19]

$$A(z) = \frac{H_{max} - H_{min}}{2r_o} \quad (1)$$

where B_{max} and B_{min} are the maximum and minimum value of the magnetic field at a distance of r_0 from the central axis. The quadrupole moment was measured along 3 pairs of

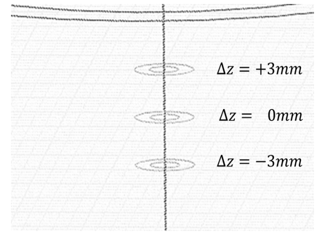

r_o [mm]	A(z) $[\frac{kA}{m^2}]$	A(z) $[\frac{kA}{m^2}]$	A(z) $[\frac{kA}{m^2}]$	RF Structure
	$z = -3mm$	$z = 0mm$	$z = +3mm$	
2	375	361	365	1.4 cell
2	1156	1259	1214	1.6 cell
4	355	382	385	1.4 cell
4	583	555	586	1.6 cell

(a) (b)

Figure 4: (a) Geometry of quadrupole moment measurement. (b) Quadrupole moment comparison table.

circles of different radii(2mm and 4mm). One pair is located at the center of the full cell and the remaining two pairs are at a distance of $\Delta z \pm 3$mm as shown in Fig 4a. Fig 4b shows the 1.4 cell gun quadrupole moment achieves up to an order of magnitude lower than the 1.6 cell gun.

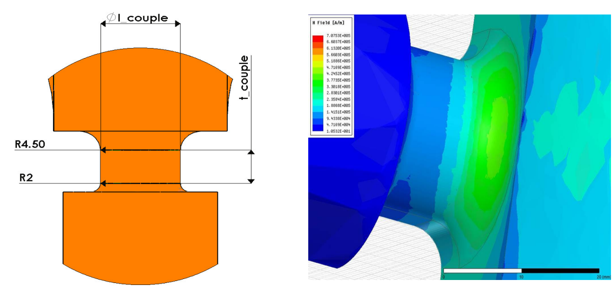

(a) (b)

Figure 5: (a) Coupling port geometry. (b)$H_{surface}$ map.

Laser ports have been placed on the first cell with rounded edges to maintain the $H_{surface} < 480$kA/m, Fig. 6b. One of the issues arising from shortening of first cell is machining these rounded edges. To ease the fabrication challenge, the first cell was truncated to create a surface normal to the laser ports as shown in Fig. 6a.

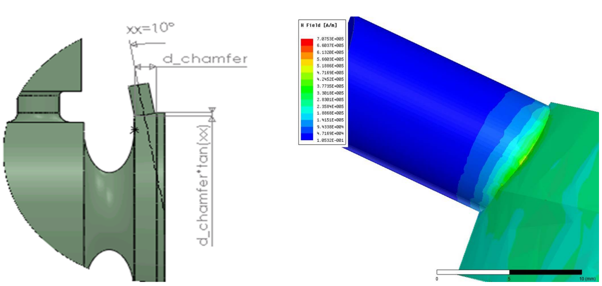

(a) (b)

Figure 6: (a) Laser ports geometry. (b)$H_{surface}$ map.

Recently it has been demonstrated that a very small drive laser spot size on the cathode generates ultra-low emittance beams, down to 5nm-rad at 20fC bunches [22]. The oblique incidence angle and laser port diameter limits how small the laser spot size can be. The current iris design restricts the illumination angle to 10^o. The numerical aperture of the

Copyright © 2016 CC-BY-3.0 and by the respective authors

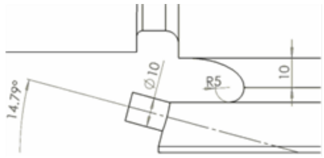

Figure 7: Oblique incidence angle solution.

ports is NA=0.083. The calculated beam waist, $w_o = \frac{\lambda_o}{\pi NA}$, is 1μm with a drive laser wavelength, λ_o, of 266nm. The laser spot projection ($w_o/tan(10^o)$) is 5.8μm in size. A possible solution to reduce the laser spot size involves a minor redesign of the iris. The first half of the iris adopts a circular geometry and the second half remains elliptically shaped, see Fig 7. This solution allows laser ports of equal length and radii as previously discussed but an increased illumination angle of 14.79^o, reducing the laser beam spot projection to 3.7μm. Further investigation is needed to implement this solution.

FABRICATION

The LNF-INFN developed a clamping technique for manufacturing the 1.6 cell photoinjector. The clamping technique avoids the brazing process for the main body of the photoinjector with the help of special gaskets that guarantee RF contact and vacuum sealing [23]. Brazing is expensive, a high risk procedure and softens the copper. Cold (not brazed) copper shows a significant improvement in breakdown probability. In Fig 8b, the clamping components are shown. The cavity is made of central piece of OFHC copper. Part 1 is an added piece for fitting of the cathode assembly. Part 2 seals the full cell using the special gasket.

New vacuum sealing gaskets were developed and tested at UCLA to completely avoid any brazing/welding of the external components onto the main body. The gaskets are made out of aluminum to act as the interface between the copper body and a standard CF flange. One side of the gasket is flat to allow the knife edge on the CF flange to bite into the aluminum [24]. The opposing side of the gasket has been patterned with a knife edge that digs onto the copper surface, pictured in Fig. 8a.

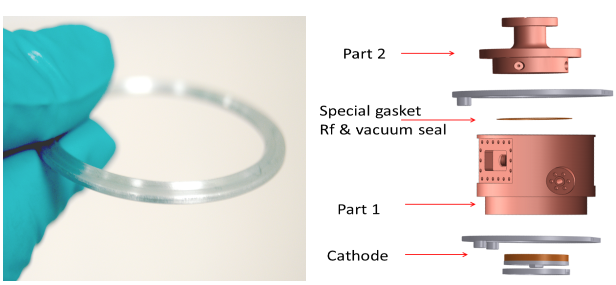

(a) (b)

Figure 8: (a)$2^{3/4}$" Aluminum gasket. (b) Clamping components.

A new feature of the 1.4 cell photoinjector is the compatibility with a load-lock chamber mechanism for the use of advanced photocathodes that have yet to be tested in high gradient structures [7]. Advanced photocathodes include alkali-antimonide photocathodes that have shown low photoemission emittance and high quantum efficiency and can open the door to extremely high peak beam brightness. Testing these photocathodes require a compact vacuum load-lock which is not commercially available. The load-lock system is currently under design and is required to deliver pregrown cathodes from their preparation chamber directly into the photoinjector without breaking vacuum.

SUMMARY

In this paper we have discussed the simple solution of shortening the first cell to minimize the phase slippage to increase the optimal launch phase to 70^o for the S-band 1.4 cell photoinjector operating at a gradient of 120 MV/m. We have presented design modifications to the SPARC S-band 1.6 cell photoinjector to improve the extraction field (and therefore higher beam brightness) by at least a factor of 1.9. The new full cell geometry was optimized to lower the quadrupole moment along the central axis achieving up to one order of magnitude lower than the SPARC gun. The 1.4 cell photoinjector fabrication approach entirely avoids any brazing and welding process by implementing the LNF-INFN clamping technique along with newly developed vacuum sealing technologies at UCLA to reduce cost, manufacturing time, preserve the hardness of cold copper and maintain a low breakdown probability. The 1.4 cell gun combines the high extraction field with a highly compact vacuum system needed to deliver and utilize pregrown AA photocathodes that promise extremely high peak beam brightness.

ACKNOWLEDGMENT

This work was partially funded by NSF grant 145583. We would like also to acknowledge V. Lollo and A. Battisti for helpful technical discussions and suggestions.

REFERENCES

[1] R. Akre, D. Dowell, P. Emma, J. Frisch, S. Gilevich, G. Hays, Ph. Hering, R. Iverson, C. Limborg-Deprey, H. Loos, A. Miahnahri, J. Schmerge, J. Turner, J. Welch, W. White, and J. Wu et al., "Commissioning the Linac Coherent Light Source injector", *Phys. Rev. ST Accel. Beams*, vol. 11, p. 030703, 2008.

[2] P. Musumeci, J. T. Moody, C. M. Scoby, M. S. Gutierrez and M. Westfall *et al.*, "Laser-induced melting of a single crystal gold sample by time-resolved ultrafast relativistic electron diffraction", *Appl. Phys. Lett.*, vol. 97, p. 063502, 2010.

[3] David J. Gibson *et al.*, *Phys. Plasmas*, vol. 11, p. 2857, 2004.

[4] Y. Shen *et al.*, "Tunable Few-Cycle and Multicycle Coherent Terahertz Radiation from Relativistic Electrons", *Phys. Rev. Lett.*, vol. 107, p. 204801, 2011.

[5] M. B. Callaham *et al.*, "Quantum-mechanical constraints on electron-beam brightness", *IEEE J. Quantum Electronics*, vol. 24, p. 1958, 1988.

Copyright © 2016 CC-BY-3.0 and by the respective authors

[6] M. Divall, E. Prat, S. Bettoni, C. Vicario, A. Trisorio, T. Schietinger, and C. Hauri *et al.*, "Intrinsic emittance reduction of copper cathodes by laser wavelength tuning in an rf photoinjector", *Phys. Rev. ST Accel. Beams*, vol. 18, p. 033401, 2015.

[7] Jared Maxson, Luca Cultrera, Colwyn Gulliford and Ivan Bazarov. *et al.*, "Thermal limit to the intrinsic emittance from metal photocathodes", *Appl. Phys. Lett.*, vol. 106, p. 234102, 2015.

[8] L. Cultrera, S. Karkare, H. Lee, X. Liu, I. Bazarov, and B. Dunham *et al.*, "Cold electron beams from cryocooled, alkali antimonide photocathodes", *PhysRevSTAB*, vol. 18, p. 113401, 2015.

[9] Jun Feng, J. Nasiatka, Weishi Wan, Siddharth Karkare, John Smedley and Howard A. Padmore, *et al.*, "Thermal limit to the intrinsic emittance from metal photocathodes", *Applied Physics Letters*, vol. 107, no. 13, p. 134101, 2015.

[10] D Velázquez, R Seibert, H Ganegoda, D Olive, A Rice, K Logan, Z Yusof, *et al.*, "Tailoring the emissive properties of photocathodes through materials engineering: Ultra-thin multilayers", *Applied Surface Science*, vol. 360, p. 762, 2016.

[11] C. Brau, in *Proceedings of the ICFA Workshop*, Chia Laguna, Sardinia, Italy, July 2002.

[12] Ivan V. Bazarov, Bruce M. Dunham, and Charles K. Sinclair *et al.*, "Maximum Achievable Beam Brightness from Photoinjectors", *Phys. Rev. Lett.*, vol. 102, p. 104801, 2009.

[13] P. Musumeci, J. T. Moody, R. J. England, J. B. Rosenzweig, and T. Tran *et al.*, "Experimental generation and characterization of uniformly filled ellipsoidal electron-beam distributions", *Phys. Rev. Lett.*, vol. 100, p. 244801, 2008.

[14] J. B. Rosenzweig *et al.*, "Next Generation High Brightness Electron Beams From Ultra-High Field Cryogenic Radiofrequency Photocathode Sources", arxiv.org/pdf/1603.01657, 2016.

[15] K. J. Kim *et al.*, "Rf and space-charge effects in laser-driven rf electron guns", *Nucl. Instr. Methods A*, vol. 275, p. 201, 1988.

[16] D. Alesini *et al.*, "New frontiers in nuclear physics with high-power lasers and brilliant monochromatic gamma beams", *Phys. Rev. STAB*, vol. 18 p. 092001, 2015.

[17] HFSS, /urlhttp://www.ansys.com

[18] F. Cardelli *et al.*, "DESIGN OF A LINAC WITH THE NEW GASKETS CLAMPING FABRICATION TECHNIQUE", in *Proceedings of IPAC2016*, Busan, Korea, p. 403.

[19] D. Alesini *et al.*, "The C-Band accelerating structures for SPARC photoinjector energy upgrade", in *Journal of Instrumentation*, Volume 8, P05004, May 2013.

[20] V.A. Dolgashev *et al.*, “High Magnetic Fields in Couplers of X-Band Accelerating Structures”, in *Proceedings of the 2003 Particle Accelerator Conference*, Portland, OR, USA, 2003.

[21] D. Alesini, "Power Coupling", CERN, Yellow Report CERN-2011- 007, 125-147, e-Print: arXiv:1112.3201 (2011).

[22] D. Cesar *et al.*, "Demonstration of Single-Shot Picosecond Time-Resolved MeV Electron Imaging Using a Compact Permanent Magnet Quadrupole Based Lens", *Phys. Rev. Lett.*, vol. 117, p. 024801, 2016.

[23] D. Alesini *et al.*,"Process for manufacturing a vacuum and radio-frequency metal gasket and structure incorporating it", Int’l patent application PCT/IB2016/051464, assigned to INFN.

[24] E.Pirez *et al.*, "S-band 1.4 cell photoinjector design for high brightness beam generation", *Nuclear Instruments Methods in Physics Research*, 2016.

Copyright © 2016 CC-BY-3.0 and by the respective authors